Influence of Inner Diameter and Height of Ring-Shaped REBaCuO Bulks on Trapped Field and Mechanical Stress During Field-Cooled Magnetization

Hiroyuki Fujishiro, Keita Takahashi, Tomoyuki Naito, Yousuke Yanagi, Yoshitaka Itoh, Takashi Nakamura, and Mark Ainslie, *Senior Member, IEEE*

***Abstract*—In this paper, the trapped field B_z, thermal hoop stress $\sigma_\theta{}^{\text{cool}}$ by cooling from 300 to 50 K, and electromagnetic hoop stress $\sigma_\theta{}^{\text{FCM}}$ during field-cooled magnetization (FCM) from $B_{\text{app}} = 6.3$ and 9.4 T are investigated numerically for ring-shaped REBaCuO bulks with various inner diameters (*I.D.*) and heights (*H*) and reinforced by an Al alloy ring. For simplicity, an identical critical current density $J_c(B)$, which is a typical value at 50 K, is assumed in the simulation. The B_z value at the center of the ring bulk changes depending on the *I.D.* and *H* values of the ring bulk, which results from the different distribution of the superconducting current. As a result, the total hoop stress $\sigma_\theta{}^{\text{total}}$ $(= \sigma_\theta{}^{\text{cool}} + \sigma_\theta{}^{\text{FCM}})$ also changes for each ring bulk and each B_{app} because of the variation of the $\sigma_\theta{}^{\text{cool}}$ and $\sigma_\theta{}^{\text{FCM}}$ values. The maximum $\sigma_\theta{}^{\text{total}}$ value, which affects the bulk fracture at $B_{\text{app}} = 9.4$ T, increases with decreasing the height of ring bulk. These results can present guidelines for designing a trapped-field magnet using ring bulks.**

***Index Terms*—Bulk high-temperature superconductors, finite element method, field-cooled magnetization, mechanical properties, numerical simulation.**

I. Introduction

FOR the practical application of trapped field magnets (TFMs) using superconducting bulks such as RE-Ba-Cu-O (REBaCuO, RE: rare earth element or Y) and MgB_2, it is an important issue to increase the trapped field in the bulk. The trapped field capability of a disk-shaped bulk is proportional to the critical current density, $J_c(B, T)$, and the diameter, as well as the height of the bulk. For field-cooled magnetization (FCM), which is a conventional magnetizing technique, increasing $J_c(B, T)$ by lowering the operating temperature is an effective way to enhance the trapped field. To date, a highest trapped field of 17.6 T has been achieved at 26 K in a disk-shaped GdBaCuO bulk pair reinforced by shrink-fit stainless steel [1]. During the FCM process, however, a large Lorentz force, $\boldsymbol{F}_{\text{L}}$ $(= \boldsymbol{J} \times \boldsymbol{B})$, is generated due to the interaction between the induced current density (J) and the magnetic field (B), and results in fracture of the bulk when the magnetic stress exceeds the mechanical strength of the material. Analytical solutions of the mechanical stresses have been investigated during FCM for the disk and ring bulks with infinite height, in which the Bean's critical state model was mainly used for superconducting characteristics [2]–[4].

A ring-shaped REBaCuO bulk is also useful for practical applications such as nuclear magnetic resonance (NMR) spectrometers and magnetic resonance imaging (MRI) apparatus [5], [6], in which the trapped field enhancement is an ongoing challenge to improve their resolution. In addition to $J_c(B, T)$, the distributions of the trapped field and mechanical stress change depending on the inner diameter (*I.D.*), outer diameter (*O.D.*) and height (*H*) of the ring bulk. Although several experimental and numerical results exist for the trapped field and mechanical stress for the ring-shaped bulk [7]–[10], there have not been systematic investigations for the mechanical stress and the effect of the metal ring reinforcement in the ring bulk with finite height.

In the present paper, the trapped field, B_z, thermal hoop stress, $\sigma_\theta{}^{\text{cool}}$, by cooling from 300 to 50 K and electromagnetic hoop stress, $\sigma_\theta{}^{\text{FCM}}$, during FCM from $B_{\text{app}} = 6.3$ and 9.4 T are investigated for ring-shaped REBaCuO bulks (*O.D.* = 64 mm) with various *I.D.* and *H* and reinforced by an aluminum (Al) alloy ring, under the assumption of an identical critical current density, $J_c(B)$, for the bulk. The influence of the shape of the ring bulk on the risk of the mechanical fracture is also discussed.

II. Numerical Simulation Framework

A three-dimensional (3D) finite element model was constructed, based on our experimental setup for FCM [8] as shown

Manuscript received October 22, 2018; accepted January 28, 2019. Date of publication January 31, 2019; date of current version February 21, 2019. This work was supported in part by JSPS KAKENHI under Grant 15K04646. The work of M. D. Ainslie was supported by an Engineering and Physical Sciences Research Council Early Career Fellowship EP/P020313/1. *(Corresponding author: Hiroyuki Fujishiro.)*

H. Fujishiro, K. Takahashi, and T. Naito are with the Department of Physical Sciences and Materials Engineering, Faculty of Science and Engineering, Iwate University, Morioka 020-8551, Japan (e-mail: fujishiro@iwate-u.ac.jp; t2216017@iwate-u.ac.jp; tnaito@iwate-u.ac.jp).

Y. Yanagi and Y. Itoh are with the IMRA Material R&D Company Ltd, Kariya 448-0032, Japan (e-mail: yanagi@ai-i.aisin.co.jp; y-itoh@ai-i.aisin.co.jp).

T. Nakamura is with RIKEN, Wako 351-0198, Japan (e-mail: ta-kashi.nakamura@riken.jp).

M. Ainslie is with the Bulk Superconductivity Group, Department of Engineering, University of Cambridge, Cambridge CB2 1PZ, U.K. (e-mail: mark.ainslie@eng.cam.ac.uk).

Color versions of one or more of the figures in this paper are available online at http://ieeexplore.ieee.org.

Digital Object Identifier 10.1109/TASC.2019.2896782

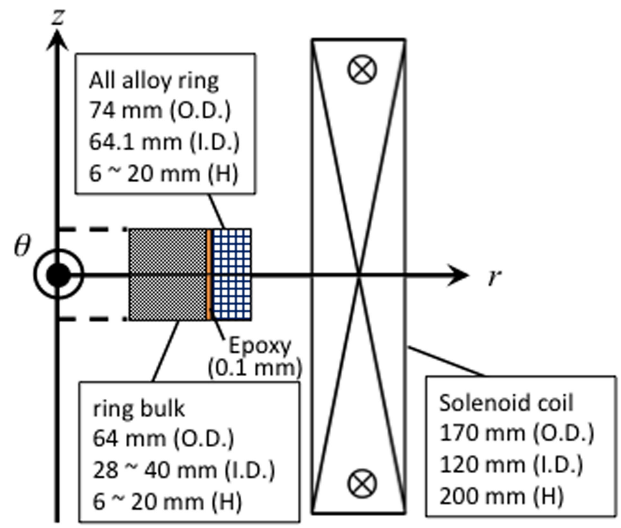

Fig. 1. Cross-sectional view of the numerical model of the ring bulk reinforced by Al alloy ring, which is magnetized using a solenoid coil.

TABLE I
DIMENSIONS OF THE FIVE SIMULATED REBACUO RING BULKS

Bulk name	O.D. (mm)	I.D. (mm)	H (mm)
Bulk (1)	64	40	20
Bulk (2)	64	28	20
Bulk (3)	64	34	20
Bulk (4)	64	34	12
Bulk (5)	64	34	6

in Fig. 1, for the electromagnetic and mechanical simulation. Five REBaCuO ring bulks 64 mm in O.D. were investigated, in which *I.D.* was changed from 28 to 40 mm and *H* was changed from 20 to 6 mm, as shown in Table I. Each ring bulk was mounted in an Al alloy (A7075-T6) ring 5 mm in width (74 mm in *O.D.* and 64.2 mm in *I.D.*) with the same height as the ring bulk using an epoxy resin 0.1 mm in thickness. In the FCM process, the ring bulk was cooled to the magnetizing temperature of $T_s = 50$ K, based on the experimental setup [5], [6], under initial applied fields of $B_{app} = 6.3$ and 9.4 T using a solenoid coil (170 mm in *O.D.*, 120 mm in *I.D.* and 200 mm in *H*), and then, the external field was decreased linearly at -0.222 Tmin^{-1} down to zero. The B_{app} value of 6.3 and 9.4 T is equivalent to 270 and 400 MHz, respectively, considering practical NMR resolution. The time step (*TS*) of the descent of the magnetic field during FCM is defined as $TS = 10$ (B_{app} - B_{ex})/B_{app} by 10 steps, in which B_{ex} is the actual time-dependent external field.

The electromagnetic phenomena during FCM are described elsewhere [10], [11]. The temperature variation during FCM is ignored for simplicity, assuming isothermal conditions. The *E-J* power law is used to simulate the highly non-linear resistivity of the superconductor, where the electric field, *E*, is proportional to J^n, and $n = 20$ is assumed as a typical value for HTS materials and a good approximation of Bean's critical state model [12]. The $J_c(B)$ characteristics of the bulk were assumed using the

TABLE II
ASSUMED MECHANICAL PARAMETERS OF REBACUO BULK, EPOXY RESIN, AND AL ALLOY USED IN THE NUMERICAL SIMULATION

	E_Y (GPa)[a]	ν[b]	α (K^{-1})[c]
REBaCuO bulk	100	0.33	6.80 x 10^{-6}
Epoxy resin	3	0.37	4.61 x 10^{-5}
Al alloy (A7075-T6)	78	0.34	1.72 x 10^{-5}

[a]Young's modulus, [b]Poisson ratio, [c]Thermal expansion coefficient.

following equation [13], [14].

$$J_c(B) = J_{c1} \exp\left(-\frac{B}{B_L}\right) + J_{c2}\frac{B}{B_{max}} \times \exp\left[\frac{1}{k}\left(1 - \left(\frac{B}{B_{max}}\right)^k\right)\right], \quad (1)$$

where each parameter ($J_{c1} = 2.3 \times 10^9$ A/m^2, $J_{c2} = 1.57 \times 10^9$ A/m^2, $B_L = 0.8$ T, $B_{max} = 4.5$ T and $k = 1.0$) can reproduce actual experimental results at 50 K [15], [16].

The co mmercial finite element method (FEM) software package, Photo-Eddy (Photon Ltd., Japan), was adapted for the analysis of the trapped field, B_z, and induced current density, J_θ, along the θ-direction in the bulk. Elastic behavior in isotropic materials can be expressed by Hooke's law, and a detailed explanation is provided elsewhere [7], [8]. The nodal force on each node of the meshed elements calculated by Photo-Eddy was exported to the software package, Photo-ELAS (Photon Ltd., Japan), for the analysis of the hoop stress, σ_θ. The assumed mechanical parameters (Young's modulus, E_Y, Poisson ratio, ν, and thermal expansion coefficient, α) of each component used in the mechanical simulation are su mmarized in Table II, which are assumed to be isotropic and to be in the elastic region.

III. RESULTS OF ELECTROMAGNETIC SIMULATION

Fig. 2(a) shows the *TS* dependence of trapped field at the center of the five ring bulks, B_z ($z = r = 0$ mm), during FCM from $B_{app} = 6.3$ T and 9.4 T. The B_z value gradually decreases with increasing *TS* for each case. For each B_{app}, the B_z value at the final step ($TS = 10$) changes depending on the *I.D.* and *H* values. For the ring bulks with identical height of $H = 20$ (bulks (1) – (3)), the final B_z value increases with decreasing *I.D.* For the bulks with identical *I.D.* = 34 mm, the final B_z value increases with increasing *H*. It should be noted that the final B_z value for bulk (5) (*I.D.* = 34 mm, $H = 6$ mm) is the same for both B_{app} values. These results suggest that the thin bulk was fully magnetized for higher B_{app} than 6.3 T and that the induced supercurrent flows through the entire bulk.

Fig. 2(b) shows the final B_z ($z = r = 0$ mm) value for the ring bulks with $H = 20$ mm for $B_{app} = 6.3$ and 9.4 T, as a function of *I.D.* B_z decreases with increasing *I.D.* Fig. 2(c) shows the final B_z ($z = r = 0$ mm) value for the ring bulks with *I.D.* = 34 mm for $B_{app} = 6.3$ and 9.4 T, as a function of *H*. B_z decreases with decreasing *H*. The thinner ring bulks cannot achieve higher trapped fields at the bulk center.

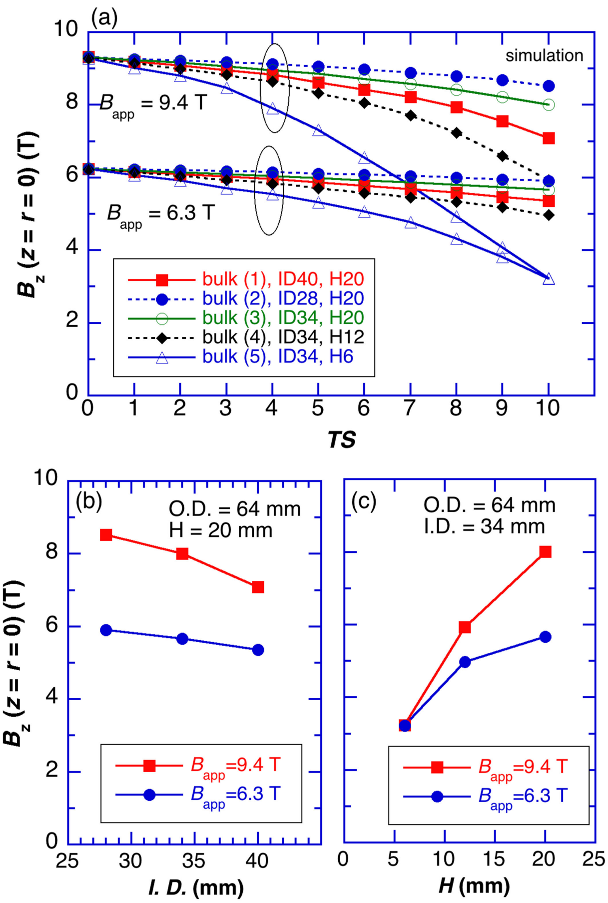

Fig. 2. (a) The *TS* dependence of the trapped field at the center of the five ring bulks, B_z ($z = r = 0$ mm), during FCM from $B_{\mathrm{app}} = 6.3$ T and 9.4 T. (b) The final B_z ($z = r = 0$ mm) value for the ring bulks with $H = 20$ mm for $B_{\mathrm{app}} = 6.3$ and 9.4 T, as a function of *I.D.* and (c) for the ring bulks with *I.D.* = 34 mm, as a function of *H*.

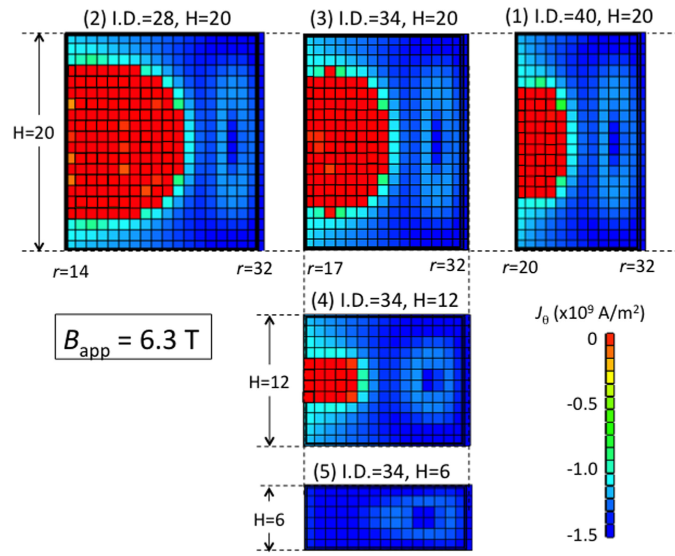

Fig. 3. Contour maps of the current density distribution along the circumferential (θ) direction for each bulk after the FCM process ($TS = 10$) from $B_{\mathrm{app}} = 6.3$ T.

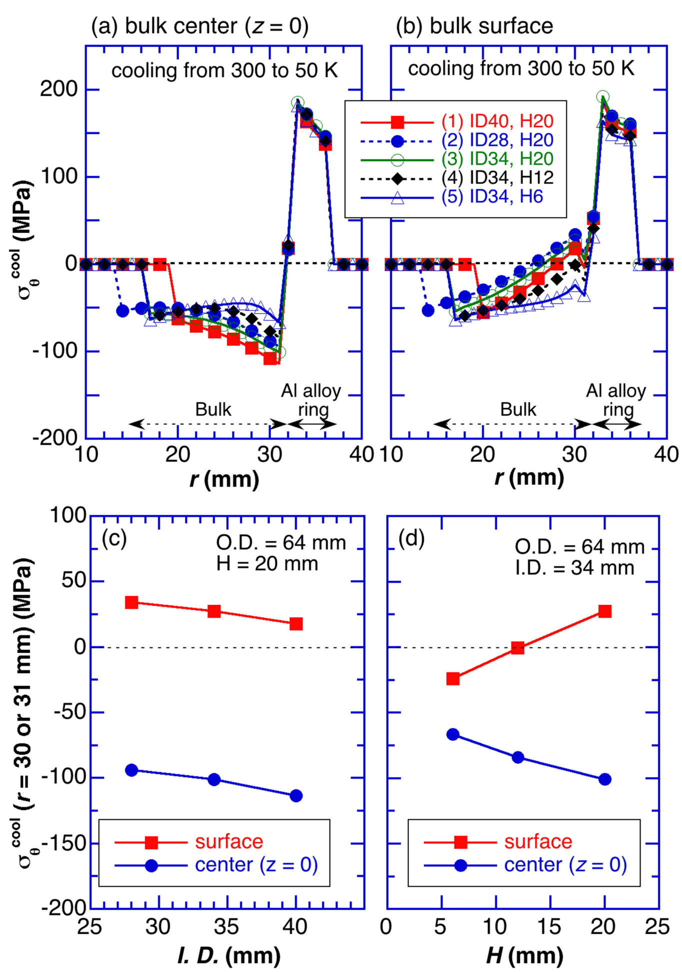

Fig. 4. Thermal hoop stress profiles, $\sigma_\theta{}^{\mathrm{cool}}$, at (a) the bulk center ($z = 0$ mm) and (b) the bulk surface, for each bulk during cooling from 300 to 50 K. (c) The $\sigma_\theta{}^{\mathrm{cool}}$ value of the ring bulks at $r = 30$ or 31 mm with $H = 20$ mm after cooling to 50 K, as a function of *I.D.* (d) The $\sigma_\theta{}^{\mathrm{cool}}$ value of the ring bulks at $r = 30$ or 31 mm with *I.D.* = 34 mm after cooling to 50 K, as a function of *H*.

Let us compare the current density distribution for each bulk during FCM. Fig. 3 shows the contour maps of the current distribution, J_θ, along the circumferential (θ) direction in each bulk after the FCM process ($TS = 10$) from $B_{\mathrm{app}} = 6.3$ T. Note that the current flows in the blue region and there is no current in the red region, as defined in Fig. 1. It was found that the current distribution changes depending on the shape of the ring bulks. For the bulks with $H = 20$ mm (bulks (1) – (3)), the supercurrent flows at the periphery and the top and bottom regions of the bulk and the no current region increases with decreasing *I.D.* On the other hand, for the bulks with *I.D.* = 34 mm (bulks (3) – (5)), no current region shrinks with decreasing *H*, and finally the supercurrent flows through the entire bulk cross-section for $H = 6$ mm. The current distribution is closely related to the trapped field profile and determines the final trapped field shown in Fig. 2(a).

IV. Results of Mechanical Simulation

A. Cooling Process

Figs. 4(a) and 4(b), respectively, show the thermal hoop stress profiles, $\sigma_\theta{}^{\mathrm{cool}}$, at the bulk center ($z = 0$ mm) and the bulk surface of each bulk after cooling from 300 to 50 K. The shape of the ring bulk influences on $\sigma_\theta{}^{\mathrm{cool}}$ profile. At the bulk center, shown in Fig. 4(a), a large compressive stress is applied to the ring bulk by the Al alloy ring due to the difference in the thermal expansion coefficient [7]. The maximum compressive stress takes place at the bulk periphery ($r = 31$ mm) for each bulk. On the other hand, on the bulk surface, as shown in Fig. 4(b), the compressive stress at the bulk periphery decreases for all the bulks and changes to a tensile stress for the bulks (1) – (3). The maximum tensile stress was +40 MPa for the smaller *I.D.* bulk (2) (*I.D.* = 28 mm, $H = 20$ mm) at $r = 31$ mm.

Fig. 4(c) shows the $\sigma_\theta{}^{\mathrm{cool}}$ value at $r = 30$ or 31 mm for the ring bulks with $H = 20$ mm after the cooling to 50 K, as a function of *I.D.* The $\sigma_\theta{}^{\mathrm{cool}}$ value decreases with increasing *I.D.* Fig. 4(d) shows the $\sigma_\theta{}^{\mathrm{cool}}$ value at $r = 30$ or 31 mm for the ring bulks with *I.D.* = 34 mm after the cooling to 50 K, as a function of H. The $\sigma_\theta{}^{\mathrm{cool}}$ value on the bulk surface changes from a positive to a negative value with decreasing H and at the bulk center ($z = 0$ mm), which has a negative (compressive) value, $\sigma_\theta{}^{\mathrm{cool}}$ decreases with decreasing H. In the ring bulk as thin as $H = 6$ mm, a compressive $\sigma_\theta{}^{\mathrm{cool}}$ is present in all bulk region, although the trapped field is smaller.

B. FCM Process

Fig. 5(a) shows the time step dependence of electromagnetic hoop stress, $\sigma_\theta{}^{\mathrm{FCM}}$, during FCM from $B_{\mathrm{app}} = 9.4$ T at the inner edge on the bulk surface for each ring bulk, at which the $\sigma_\theta{}^{\mathrm{FCM}}$ value is the maximum in each bulk [7], [9]. $\sigma_\theta{}^{\mathrm{FCM}}$ increases with increasing *TS*, takes a maximum at an intermediate *TS* and then decreases with the increase in *TS* for each ring bulk, which is a co mmon tendency for $\sigma_\theta{}^{\mathrm{FCM}}$ during FCM. It should be noted that the $\sigma_\theta{}^{\mathrm{FCM}}$ – *TS* profile for bulk (5) (*I.D.* = 34 mm, $H = 6$ mm) is quite different to that for the other bulks because the supercurrent flows through the entire bulk cross-section.

Fig. 5(b) shows the maximum electromagnetic hoop stress, $\sigma_\theta{}^{\mathrm{FCM}}$(max), as a function of *I.D.,* for the bulks with $H = 20$ mm, at the bulk center and the bulk surface, during FCM from 6.3 and 9.4 T. $\sigma_\theta{}^{\mathrm{FCM}}$(max) occurs at the inner edge of each ring bulk and at the bulk surface this is slightly larger than at the bulk center ($z = 0$ mm). Fig. 5(c) shows $\sigma_\theta{}^{\mathrm{FCM}}$(max) in the bulks of *I.D.* = 34 mm at bulk center and bulk surface during FCM, as a function of H. Similar to Fig. 5(b), the difference between the bulk center and bulk surface is very small. $\sigma_\theta{}^{\mathrm{FCM}}$(max) increases with decreasing H, which suggests that the thin ring bulk fractures more easily during FCM.

B. Cooling + FCM Process

Figs. 6(a) and 6(b), respectively, show the *TS* dependence of the total hoop stress profile, $\sigma_\theta{}^{\mathrm{total}}$ ($= \sigma_\theta{}^{\mathrm{cool}} + \sigma_\theta{}^{\mathrm{FCM}}$), for bulk (3) (*I.D.* = 34 mm, $H = 20$ mm) at the bulk center ($z = 0$ mm) and at the bulk surface ($z = 10$ mm) during FCM from 9.4 T. The $\sigma_\theta{}^{\mathrm{total}}$ profile at the step 0 shows the $\sigma_\theta{}^{\mathrm{cool}}$ without FCM, as shown in Fig. 4. The maxmum $\sigma_\theta{}^{\mathrm{total}}$ at the bulk center ($z = 0$ mm) occurs at the inner edge ($r = 17$ mm) due to the increase from $\sigma_\theta{}^{\mathrm{FCM}}$. On the other hand, on the bulk surface ($z = 10$ mm), the maximum $\sigma_\theta{}^{\mathrm{total}}$ takes place at the inner edge ($r = 17$ mm) and also at the bulk edge ($r = 30$ mm).

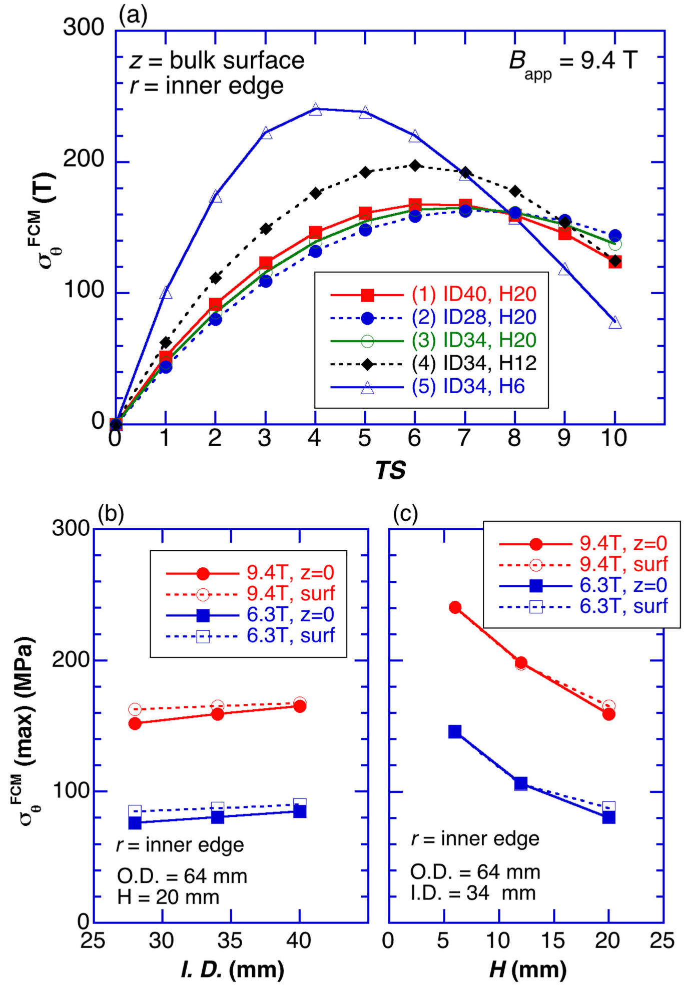

Fig. 5. The *TS* dependence of the electromagnetic hoop stress, $\sigma_\theta{}^{\mathrm{FCM}}$, during FCM from 9.4 T, at the inner edge on the bulk surface for each ring bulk. (b) Maximum electromagnetic hoop stress, $\sigma_\theta{}^{\mathrm{FCM}}$(max), in the bulks with $H = 20$ mm, at the bulk center and bulk surface during FCM, as a function of *I.D.* (c) $\sigma_\theta{}^{\mathrm{FCM}}$(max) in the bulks of *I.D.* = 34 mm at the bulk center and bulk surface during FCM, as a function of H.

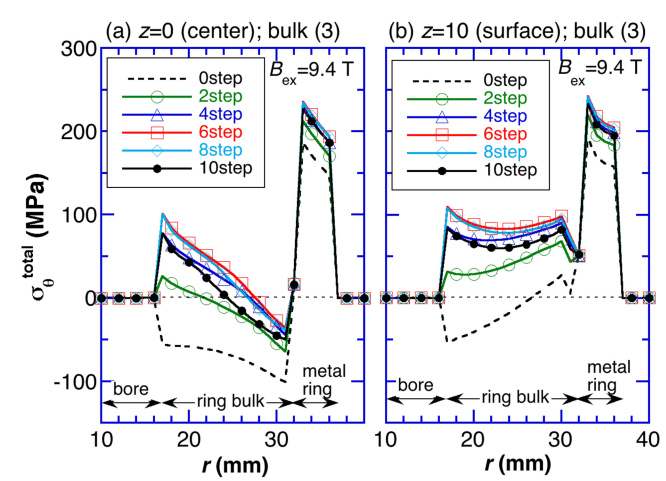

Fig. 6. The *TS* dependence of the total hoop stress profile, $\sigma_\theta{}^{\mathrm{total}}$ ($= \sigma_\theta{}^{\mathrm{cool}} + \sigma_\theta{}^{\mathrm{FCM}}$), for bulk (3) at (a) the bulk center ($z = 0$ mm) and (b) the bulk surface during FCM from 9.4 T.

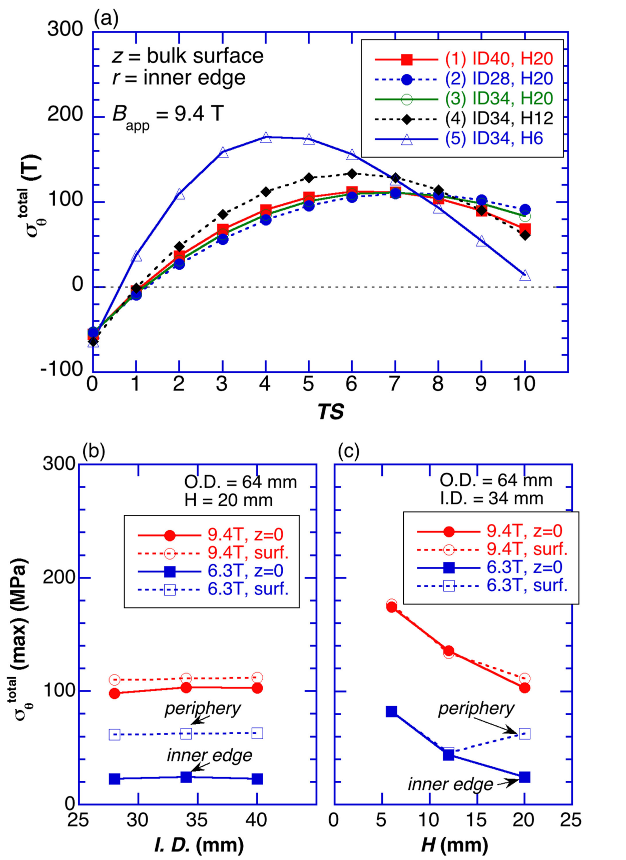

Fig. 7. (a) The *TS* dependence of the total hoop stress, $\sigma_\theta{}^{\rm total}$, at the inner edge on the bulk surface for each ring bulk during FCM from $B_{\rm app} = 9.4$ T after cooling to 50 K. (b) The maximum $\sigma_\theta{}^{\rm total}$ value for the ring bulks with $H = 20$ mm at the bulk center ($z = 0$ mm) and the bulk surface during FCM from 6.3 and 9.4 T, as a function of *I.D.* (c) The maximum $\sigma_\theta{}^{\rm total}$ value for the ring bulks with *I.D.* $= 34$ mm at the bulk center and the bulk surface during FCM, as a function of *H*.

The maximum $\sigma_\theta{}^{\rm total}$ changes depending on the *TS* dependence of the $\sigma_\theta{}^{\rm cool}$ and $\sigma_\theta{}^{\rm FCM}$ values.

Fig. 7(a) shows the *TS* dependence of the total hoop stress, $\sigma_\theta{}^{\rm total}$, at the inner edge on the bulk surface for each ring bulk during FCM from $B_{\rm app} = 9.4$ T, after cooling to 50 K. The $\sigma_\theta{}^{\rm total}$ values decreased, compared to the $\sigma_\theta{}^{\rm FCM}$ values, due to the addition of the compressive stress by cooling. However, a tensile stress larger than +100 MPa is present during FCM from 9.4 T, which suggests the possibility of the bulk fracturing, since the fracture strength of typical Ag-doped REBaCuO bulks is considered to be 50 ∼ 70 MPa [17], [18].

Fig. 7(b) shows the maximum $\sigma_\theta{}^{\rm total}$ value for the ring bulks with $H = 20$ mm at the bulk center ($z = 0$ mm) and the bulk surface during FCM from 6.3 and 9.4 T, as a function of *I.D.* The maximum $\sigma_\theta{}^{\rm total}$ for $B_{\rm app} = 9.4$ T takes place at the inner edge and the difference is small between the bulk center and surface. However, for $B_{\rm app} = 6.3$ T, the maximum $\sigma_\theta{}^{\rm total}$ value at the bulk surface is larger than that at the bulk center, because the $\sigma_\theta{}^{\rm total}$ value at the periphery of the bulk surface becomes large due to the existence of the tensile stress during the cooling process. Fig. 7(c) shows the maximum $\sigma_\theta{}^{\rm total}$ value for the ring bulks with *I.D.* $= 34$ mm at the bulk center ($z = 0$ mm) and the bulk surface during FCM from 6.3 and 9.4 T, as a function of *H*. For a similar reason to that for bulk (3), the maximum $\sigma_\theta{}^{\rm total}$ value at the bulk surface is larger than that at the bulk center for $B_{\rm app} = 6.3$ T. However, for smaller *H* values, the maximum $\sigma_\theta{}^{\rm total}$ value takes place at the inner edge and the difference between the bulk center and the bulk surface is very small.

The results in Figs. 7(b) and 7(c) suggest that the ring bulks reinforced by Al alloy ring, except bulk (5), may avoid mechanical fracture during FCM from 6.3 T, because the maximum $\sigma_\theta{}^{\rm total}$ value is +62 MPa, which is nearly the same as the fracture strength (50 ∼ 70 MPa) of typical REBaCuO bulks [17], [18]. However, bulk (5) during FCM from 6.3 T, and all five bulks during FCM from 9.4 T, must suffer fracture based on the present simulation.

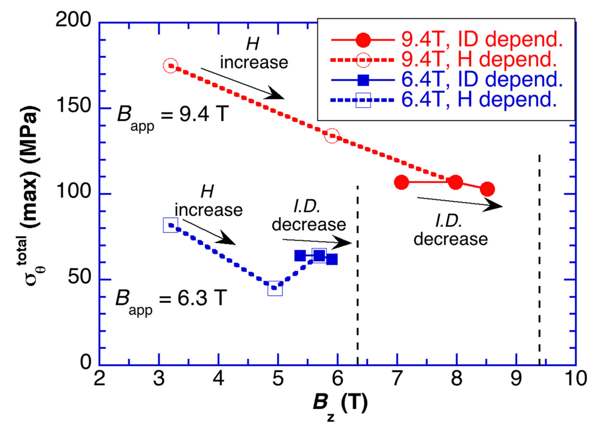

Fig. 8. The relationship between the B_z value and the $\sigma_\theta{}^{\rm total}$(max) value for the five cases at $B_{\rm app} = 6.3$ and 9.4 T.

Fig. 8 shows the relationship between the trapped field, B_z, and the maximum total hoop stress, $\sigma_\theta{}^{\rm total}$(max), for the five ring bulks for $B_{\rm app} = 6.3$ and 9.4 T, which was summarized from Figs. 2(a) and 7. It was found that the *I.D.* should be decreased and *H* should be increased to both enhance the trapped field and reduce the hoop stress simultaneously. This direction means the approach to fabricating a long disk bulk. These results present useful guidelines for designing ring-shaped TFMs to avoid the mechanical fracture. However, to achieve a higher trapped field during FCM from $B_{\rm app} = 9.4$ T without fracture, a new reinforcement method must be applied [10].

IV. Conclusion

We have investigated numerically the trapped field, B_z, thermal hoop stress, $\sigma_\theta{}^{\rm cool}$, by cooling from 300 to 50 K and electromagnetic hoop stress, $\sigma_\theta{}^{\rm FCM}$, during FCM from $B_{\rm app} = 6.3$ and 9.4 T for ring-shaped REBaCuO bulks of various *I.D.* and *H*, reinforced by an Al alloy ring. The total hoop stress $\sigma_\theta{}^{\rm total}$ ($= \sigma_\theta{}^{\rm cool} + \sigma_\theta{}^{\rm FCM}$) changed at each position and for each $B_{\rm app}$ due to variation of $\sigma_\theta{}^{\rm cool}$ and $\sigma_\theta{}^{\rm FCM}$. The maximum $\sigma_\theta{}^{\rm total}$ value, at the innermost edge decreases with increasing the height of ring bulk. For $B_{\rm app} = 6.3$ T, the maximum $\sigma_\theta{}^{\rm total}$ value can be reduced below the fracture strength of 50 ∼ 70 MPa of the bulk material. However, for $B_{\rm app} = 9.4$ T, the ring bulk must break. It is necessary to introduce a new reinforcement structure to avoid the mechanical fracture of the ring bulk to realize the 400 MHz NMR bulk magnet.

REFERENCES

[1] J. H. Durrell *et al.*, "A trapped field of 17.6 T in melt-processed, bulk Gd-Ba-Cu-O reinforced with shrink-fit steel," *Supercond. Sci. Technol.*, vol. 27, 2014, Art. no. 082001.

[2] T. H. Johansen, C. Wang, Q. Y. Chen, and W.-K. Chu, "Enhancement of tensile stress near a hole in superconducting trapped-field magnets," *J. Appl. Phys.*, vol. 88, pp. 2730–2733, 2000.

[3] T. H. Johansen, Q. Y. Chen, and W.-K. Chu, "Pinning-induced stress in clamped superconductors," *Physica C*, vol. 349, pp. 201–210, 2001.

[4] T. M. Johansen, "Flux-pinning-induced stress and magnetostriction in bulk superconductors," *Supercond. Sci. Technol.*, vol. 13, pp. R121–R137, 2000.

[5] T. Nakamura, Y. Itoh, M. Yoshikawa, T. Oka, and J. Uzawa, "Development of a superconducting magnet for nuclear magnetic resonance using bulk high-temperature superconducting materials," *Concepts Magn. Reson. B*, vol. 31B, pp. 65–70, 2007.

[6] T. Nakamura *et al.*, "Development of a superconducting bulk magnet for NMR and MRI," *J. Mag. Reson.*, vol. 259, pp. 68–75, 2015.

[7] H. Fujishiro *et al.*, "Simulation studies of mechanical stresses in REBaCuO superconducting ring bulks with infinite and finite height reinforced by metal ring during field-cooled magnetization," *Supercond. Sci. Technol.*, vol. 30, 2017, Art. no. 085008.

[8] K. Takahashi, H. Fujishiro, T. Naito, Y. Yanagi, Y. Itoh, and T. Nakamura, "Fracture behavior by magnetic stress in EuBaCuO superconducting ring bulk reinforced by a stainless steel during field-cooled magnetization," *Supercond. Sci. Technol.*, vol. 30, 2017, Art. no. 115006.

[9] K. Takahashi, H. Fujishiro, T. Naito, Y. Yanagi, Y. Itoh and T. Nakamura, "Numerical simulation of electromagnetic and thermal hoop stresses in REBaCuO superconducting ring and disk bulks reinforced by stainless steel ring with various thicknesses during field-cooled magnetization," *IEEE Trans. Appl. Supercond.*, vol. 28, no. 3, Apr. 2018, Art. no. 6800705.

[10] H. Fujishiro, K. Takahashi, T. Naito, Y. Yanagi, Y. Itoh, and T. Nakamura, "A new proposal of mechanical reinforcement structures to annular REBaCuO bulk magnet for compact and cryogen-free NMR spectrometer," *Physica C*, vol. 550, pp. 52–56, 2018.

[11] H. Fujishiro and T. Naito, "Simulation of temperature and magnetic field distribution in superconducting bulk during pulsed field magnetization," *Supercond. Sci. Technol.*, vol. 23, 2010, Art. no. 105021.

[12] M. D. Ainslie, D. Zhou, H. Fujishiro, K. Takahashi, Y.-H. Shi, and J. H. Durrell, "Flux jump-assisted pulsed field magnetization of high-J_c bulk high-temperature superconductors," *Supercond. Sci. Technol.*, vol. 29, 2016, Art. no. 124004.

[13] M. Jirsa, L. P°ust, D. Dlouhý, and M. R. Koblischka, "Fishtail shape in the magnetic hysteresis loop for superconductors: Interplay between different pinning mechanisms," *Phys. Rev. B*, vol. 55, pp. 3276–3284, 1997.

[14] M. Muralidhar, N. Sakai, M. Jirsa, N. Koshizuka, and M. Murakami, "Direct observation and analysis of nanoscale precipitates in (Sm,Eu,Gd)Ba2Cu3Oy," *Appl. Phys. Lett.*, vol. 85, pp. 3504–3506, 2004.

[15] M. D. Ainslie and H. Fujishiro, "Modelling of bulk superconductor magnetization," *Supercond. Sci. Technol.*, vol. 28, 2015, Art. no. 053002.

[16] T. Kii *et al.*, "Low-temperature operation of a bulk HTSC staggered array undulator," *IEEE Trans. Appl. Supercond.*, vol. 22, no. 3, Jun. 2012, Art. no. 4100904.

[17] D. Lee and K. Salama, "Enhancements in current density and mechanical properties of Y-Ba-Cu-O/Ag composites," *Jpn. J. Appl. Phys.*, vol. 29, pp. L2017–L2019, 1990.

[18] K. Katagiri *et al.*, "Effects of Ag content on the mechanical properties of (Nd,Eu,Gd)–Ba–Cu–O bulk superconductors," *Physica C*, vol. 392-396, pp. 526–530, 2003.